Evolution of the Canadian Operational Radar Network

Paul Joe[1] and Steve Lapczak[2]

National Radar Project, Environment Canada, 4905 Dufferin St., Toronto, Ontario, M3H 5T4

Abstract

The Meteorological Service of Canada began to revitalize its weather radar network in April 1997 with work scheduled to be completed in 2004. The three main components of this work include: the addition of eleven new radars and adding Doppler capability to the existing network of nineteen radars; development of processing software to support weather forecasting and quantitative precipitation estimation; and the establishment of the logistical support to the network. The radar hardware was constructed from commercial off the shelf components. One of the key concepts behind the design of the system is a networked radar system. What constitutes a network in a diverse geographical, meteorological, and operational environment was a challenge.

By the end of the summer of 2002 the network upgrade will be 90% complete. Both new and upgraded radars use the identical transmitter/receivers and signal processing providing the uniformity that was previously lacking in the network. Subject to antenna limitations, the new and upgraded radars have the same performance. The radars are more sensitive and more stable than before. Phase noise errors in Doppler mode are measured on an external target as being less than 0.4 degrees out to a range of 120km. The overall minimum detectable signal is much less than -31.5 dBZ at a range of 1 km (limited by data resolution). The radars operate with dual PRF and random phase capability while in Doppler mode. The radars operate in remote, unmanned locations. The design of the operation of the network takes full advantage of the wide area TCP/IP network (ECONET). Data are sent from the radars to regional weather centres for processing. The network is monitored in real-time to automatically detect and identify problems and real-time statistics of network performance are available.

Forecasting services in Canada are provided on a regional basis. One forecaster may have to monitor 5 to 10 Canadian radars and an equivalent number of US Nexrad radars - an area of about 3×10^6 km^2. Multiple radars are processed at regional centres using a network of PC based LINUX computers. The processing is distributed intra- and inter-regionally. The newest version of the software (known as CARDS which stands for CAnadian Radar Decision Support system) presents radar information as a composite view of multiple radars with drill down capability to ranked and classified storm cells thus providing significant analysis support to the forecasters. This support includes cell identification, multi-radar cell merging, tracking, movement forecasting, cell severity analysis and prioritization. Access to these products is through a JAVA based viewer and can operate on a variety of platforms - from high-end scientific workstations to office technology computers.

The project is still continuing and further work will be conducted in network calibration, network radar data processing and different scan strategies. The next major release of the software will focus on improvements in the quantitative precipitation estimation. Though, the project is implementing Doppler technology into operations, the growth path is towards dual polarization capability. This latter capability is being planned for installation on the King City research-operational radar.

1. Introduction

The Meteorological Service of Canada is implementing a network of thirty C Band Doppler radars (Lapczak et al, 1998). The project began in 1997 and will end in 2003. It updates an existing network of sixteen conventional and four Doppler radars. Eleven new radars are being added and the existing radars are being upgraded. As the radars are installed, they are commissioned into operations, resulting in a mixed network of Doppler and conventional volume scanning radars during the life of the project. The radar locations were selected with the intention of taking advantage of bordering Nexrad radars (Fig. 1). There are several instances where NEXRAD coverage is substantial. A prime example is extreme southwest Ontario which is bounded on three sides by Nexrad radars.

The network expansion was justified, not only on the traditional use for severe weather forecasting, but had to support several other mandates. These additional mandates include the use of radar for hydrology, climate applications, numerical weather prediction/data assimilation, environmental monitoring and

[1] *Corresponding author: Paul Joe, Tel: 416-739-4884 Email: paul.joe@ec.gc.ca*
[2] *Project Contact: Steve Lapczak Tel: 416-739-???? Email: steve.lapczak@ec.gc.ca*

commercial applications, such as aviation. While weather radars have been used for these purposes on an *ad hoc* basis, these are now recognized as part of their primary purpose.

An in-house approach to integrating radar hardware components was adopted. All new and existing non-Doppler radars are being fitted with identical transmitters/receivers and processing systems. In addition, many of the existing radars are being moved to new locations.

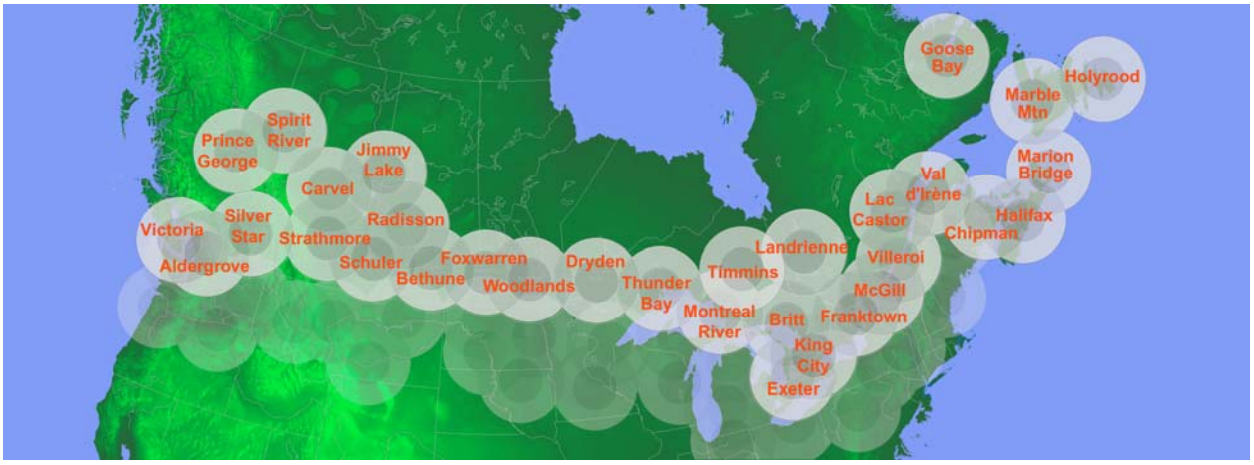

Figure 1: A map of the radar network as it is planned for completion in 2004. The shading indicates 120km and 240km range rings. Nexrad radars are shown in darker shades.

The in-house approach was also used in developing the radar data processing in order to provide an evolving development process. There had been several prototype systems already developed in Canada. Increasingly, other data sets need to be integrated with the radar data to provide decision support capability. Also, the requirements for many of the new mandates are still evolving and are not, as yet, well defined. The radar processing software was developed in a phased approach.

The first version of the software was based on the research-operational processing system used at the King City radar. This was modified to meet operational maintenance requirements and was implemented to process the first two project radar installations. The second version of the software addressed Y2K issues and was implemented right across the country. The most recent version of the software, called the Canadian Radar Decision Support (CARDS) system, focuses on the needs of the summer severe weather forecaster. Highlights of this system will be described later in this paper.

2. Radar Characteristics

The characteristics of the radars are presented in Table 1. For upgraded radars, the existing towers and antennae were retained. The new antennae are larger and have a 0.65^{o} .beam width. The small beamwidth was chosen to detect shallow weather echoes by using low elevation scans (Fig. 2). The smaller beamwidth also extends the detection range of the radar by increasing the antenna gain and hence improves sensitivity. All of these features are key factors in the long-range detection of shallow snowfall in winter weather applications.

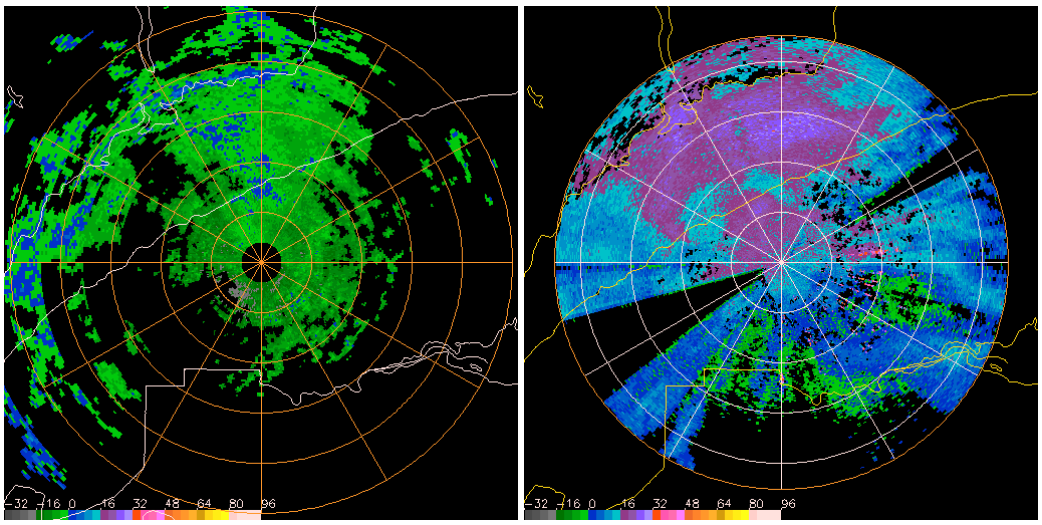

Figure 2: The left image shows a "traditional" 1.0 km CAPPI (dBZ units, 0.5 km pixels, maximum range ring is at 125km) where weather echo is sparse. On the right, a -0.5° PPI image (maximum range ring is at 113 km) shows much greater extent of the weather echo. This latter image shows the combined effectiveness of the smaller beamwidth and the FFT Doppler ground clutter filter to remove the ground echoes.

The radar transmitter and modulator have multi-pulse capability (0.8, 1.6, 2.0 and 5.0 μs) although only two are being used operationally at this time. The long pulse is designed for clear air detection. Initially we considered a 10 μs pulse but had troubles finding a good match between the modulator and magnetron. Various sampling and filtering strategies (from 8 to 2048 pulses) were tested but the greatest effect on clear air detection was the pulse width (Fig. 3). However, the sample size and the design of the matched filter also play a role in the quality of the data and in the ability to detect the clear air echoes. While in clear air mode, the pulse repetition frequency is reduced to maintain the duty cycle, thus, the Nyquist velocity is quite low and Doppler ground clutter filtering is not effective. Also, the long pulse with its poorer range resolution makes the ground echoes even more evident.

Fig. 3 shows test results from the Strathmore radar which is located on the Prairies just east of the Rocky Mountains and is a particularly good location for the detection of clear air echo. Using the 5 μs pulse, clear air echoes with reflectivity values of -16 dBZ can seen out to a range of 125 km and to a range of 75 km with the shortest pulse. Another factor in the ability to see the clear air is the target itself. Part of the reason for the range limitation at the 5 μs pulse is that the clear air target is confined to the boundary layer and the beam overshoots the echo at long ranges.

A solid state modulator is used to enhance reliability and to improve performance. A digital IF receiver was acquired from Sigmet Inc. Its implementation reduced the cost of Dopplerization of the radar, while, at the same time, provided greater linear dynamic range (>90 dB) precluding the need for a logarithmic receiver. Also the phase noise stability which determines the ground echo clutter rejection capability was dramatically improved. Phase noise measurements on external ground targets have been measured as low as 0.4° and as low as 0.2° using a microwave delay line (Fig. 4). The digital IF can achieve this high level of performance but the quality of the STALO is the critical item. We have found that analogue STALO's can vary in quality. We currently use a digitally controlled or synthesized STALO to achieve consistently good phase stability.

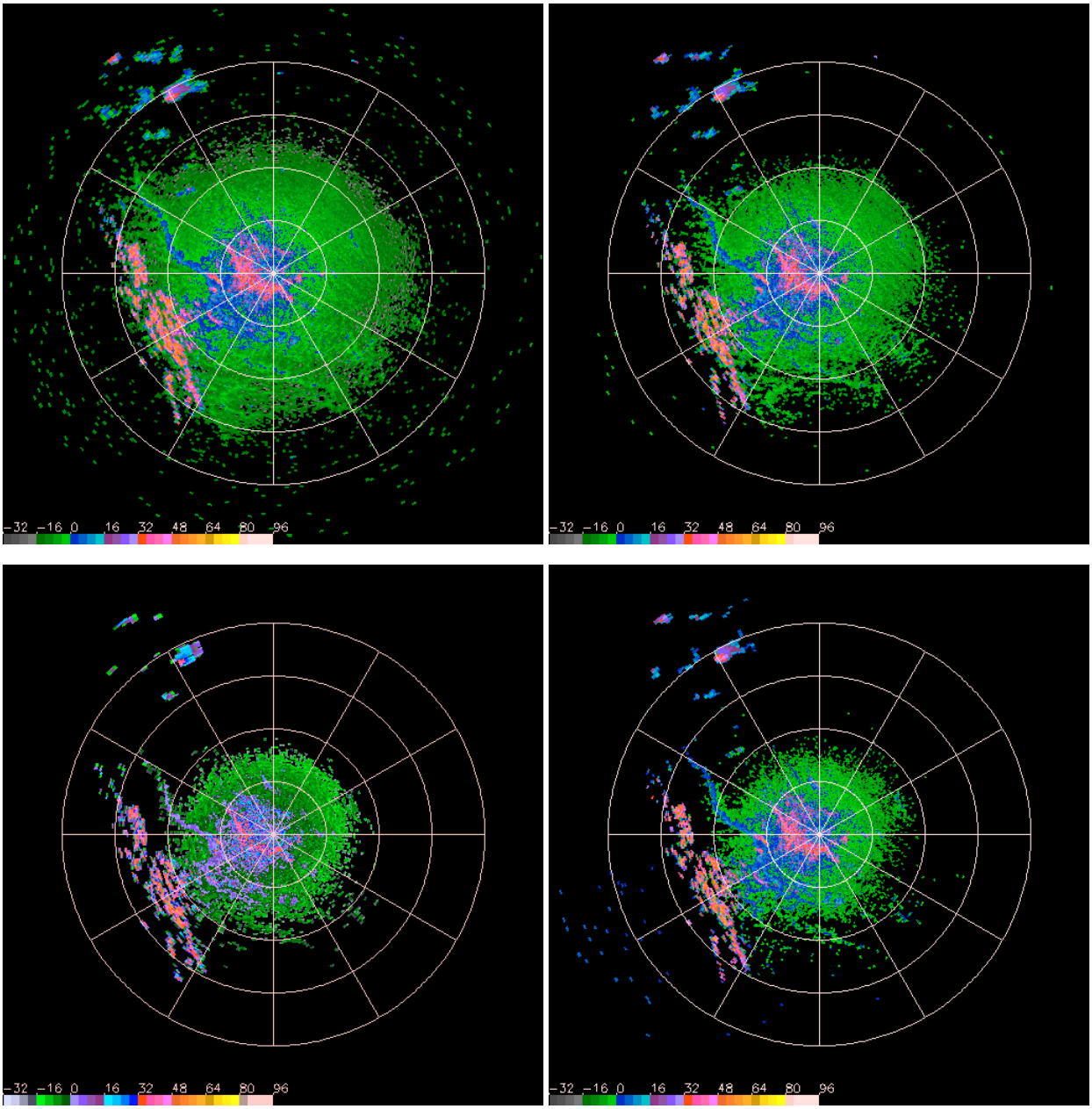

Figure 3: Clear air returns at 4 different pulse widths (5.0, 2.0,1.27 and 0.8 μs, left to right and top to bottom, respectively). The rings are at fifty-kilometer intervals. The strong echoes in the southwest are ground returns from the Rocky Mountains. A clear air boundary is observed lying approximately parallel to the mountains and to the WNW of the radar. Weather echoes due to thunderstorms are to the NNW at 200 km range. The areal coverage, indicative of sensitivity, of the clear air is mainly determined by the pulse width. (Note: the 1.27μs was not calibrated when this data was taken and shows lower reflectivities.)

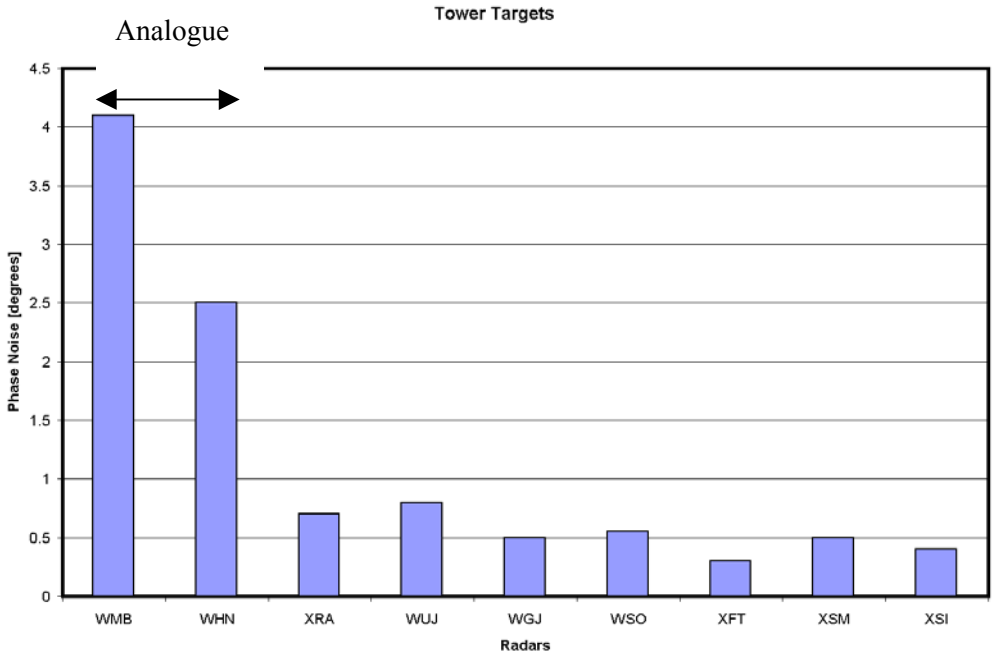

Figure 4: Phase noise measurements on external target (tower) as a function of range. The high phase noise figures are from radars with poor STALO's.

Another performance metric is the minimum detectable signal (MDS) of the radar (Fig. 5). The MDS varies slightly from radar to radar due to different tower heights, antenna gain, coupler losses, etc. Fig. 5 shows the results for the 2 μs pulse. There are four pulse widths, with different matched filters. For example, the Strathmore radar (XSM) has a MDS for 0.8, 2.0 and 5.0 μs pulses are -40.9, -47.8 and -56.2 dBZ at 1 km, respectively.

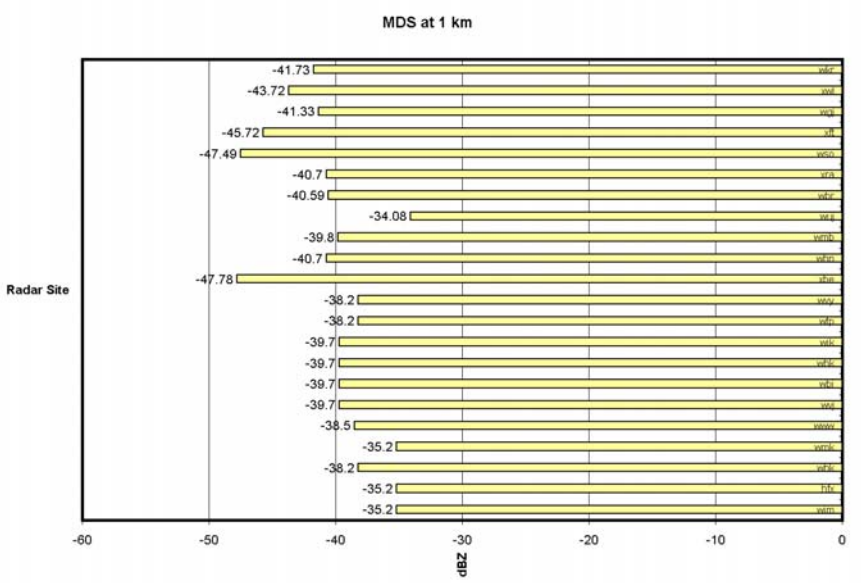

Figure 5: Minimum detectable signal (MDS) at 1km range in units of dBZ for various network radars. The signal processor reports reflectivity values greater than -31.5 dBZ. This is for the 2 μ pulse. Differences are primarily due to antenna dish size.

Table 1: Radar Characteristics

	NRP New Radar		NRP Retrofit Radar	
Antenna				
Diameter (m)	6.1		3.6	
Beamwidth	0.62°		1.1°	
Gain (dB)	49.2		43.0	
Polarization	H			
Side lobes	-26 dB: 0 to 10° <-26 dB 10° to 30° <-45 dB >30°		-23 dB 0° to 12° <-23 dB 12° to 30° <-40 dB >30°	
Elevation limits	-2 to +90		-1 to +60	
Maximimum Velocity Az	+/- 36 °/s		+/- 40 °/s	
El	0 - 15 °/s		0 - 15 °/s	
Conventional scan	36 °/s			
Doppler scan (typical)	5.1 °/s			
Transmitter				
Type	Coaxial magnetron			
Band	C			
Frequency (GHz)	5.600-5.650			
Wavelength (cm)	5.32			
Peak Power (kW)	250			
Pulse Length (μs)	0.8	2.0	0.8	2.0
PRF (Hz) - maximum	1200	250	1200	250
Receiver				
Type	Sigmet RVP7			
A/D Converter (bits)	12 or 14			
Max No. of range Gates	2048			
Min Bin spacing (m)	125			
IF 3db Bandwidth (MHz)	1.0	0,6	1.0	0,6
Phase noise (deg)	< 0.4 @ 100km			
Clutter suppression (db)	30			
Zmin (dBZ)@ 1km	< -40		< -33	

The radar site processor is the IRIS software package from Sigmet, Inc. including a four board RVP7 with FFT and random phase capability (Joe et al, 1999). It offers the functionality and flexibility required and various scan strategies can be programmed.

As the network transitions to full Doppler capability by 2003, there is a mix of Doppler and non-Doppler radars. At the moment, the scan strategy varies from 24 elevation angle reflectivity-only scans, to

multiple elevation angle Doppler scans. There are many users of the radar data that need to have regularly scheduled products from the radar network and their requirements govern the scan strategy used. The critical need is long range volume scanning to 256 km. Random phase processing was tested to extend the Doppler range to greater than 113 km. Fig. 6 shows an example where this works very well. The figure shows a well-developed mesocyclone signature at around 215 km range well into the second trip echo. The data is collected using a PRF of 1200 s^{-1} with a Nyquist of 16 m/s. The first trip ends at 126 km and the second trip ends at 226 km. The random phase scanning also improves the data quality within the first trip. While effective, not all the echo in the second trip is recoverable and alternative strategies continue to be evaluated to better meet the requirements.

When the network becomes fully Dopplerized, the target requirement is that the radar will conduct volume scans out to a range of 240 km with Doppler capability on a five minute cycle. Currently, there are a limited number of Doppler scans combined with a twenty-four elevation conventional volume scan (Marshall and Ballantyne, 1978). The latter scan strategy has been used for over twenty years and provides great detail in the vertical. In addition, strategies that take advantage of the Doppler capability to remove ground clutter (requiring many samples and hence longer scan times) in combination with the target requirements are unresolved but are actively being studied. One particular test has been conducted on an aggressive 5:4 dual PRF with a maximum range of 240 km operating on a five-minute cycle. Table 2 shows how the scanning is done now and the scan strategy that was trialed. Fig. 7 shows a comparison of the results. Data collected at a 5:4 ratio results in very noisy data due to the small difference between the individual Nyquist velocities. However, a despiking technique is used to correct the noisy data (Joe and May, 2002; May and Joe, 2001). The final result is much better than the unfiltered data but it may not be good enough for mesocyclone or microburst detection algorithms that look for shear in the radial velocity field. While very encouraging, more testing and processing is required.

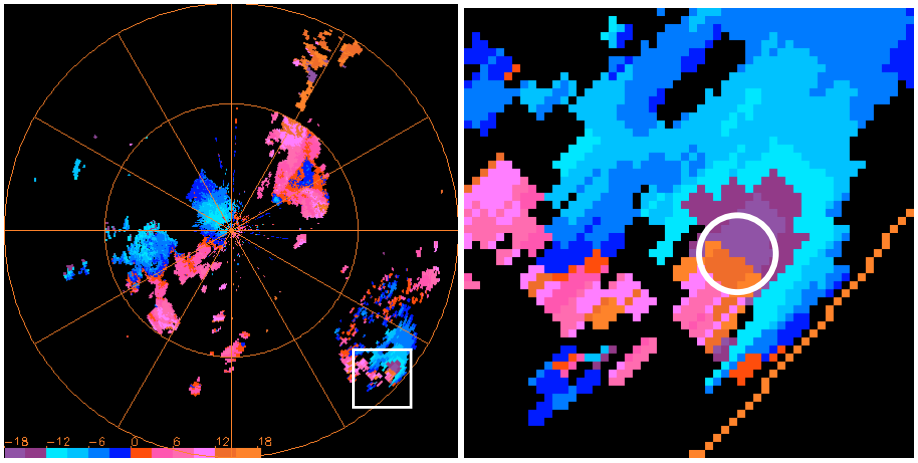

Figure 6: Radial velocity images of the Pine Lake storm. The images are from a 0.3° PPI conical surface taken with random phase processing. The left image is a full-scaled image at 0240Z 15 July 2000 and the right image is zoomed in. The inner ring is at 126 km, the limit of the first trip echo, and the outer ring is at 226 km, the limit of the second trip echo recovery. The box (left mage) highlights the mesocyclone located in the "second trip". The Nyquist velocity is 16 m/s. The patchiness in the image is a result of "unretrievable" second trip echo. The circle (right image) indicates the location of the mesocyclone identified by a couplet of away and toward velocities aligned across a radar azimuth.

Table 2: Scan Strategy Testing - Scan Characteristics

	Current			Trial		
Scan Name	**CONVOL**	**DOPVOL**	**DOPVOL2**	**NEWLOW**	**NEWVOL**	**Clearair**
Rotation rate	6 rpm	1.5 rpm	3 rpm	1.25 rpm	3.2 rpm	0.83 rpm (0.5°/s)
Pulse Width	2 μs	0.8 μs	0.8 μs	1.6 μs	1.6 μs	5 μs
Samples	8 samples	64 samples	32 samples	64	25	16-2048
Range Res.	1 km	0.5 km	1 km	0.25 km	0.25 km	0.25 km
Az Res	1.0°	0.5°	1.0°	1.0°	1.0°	1.0°
PRF	250	1192:896	1200	600:480	600:480	50
PRF Ratio	1	4:3	1	5:4	5:4	1
Nyquist	N/A	16:12 m/s	16 m/s	8.0:6.4	8.0:6.4	N/A
Ext. Nyquist	N/A	48 m/s	16 m/s	32 m/s	32 m/s	N/A
Parameters	Zt	Zt, Zc, Vr, σ_w	Zt, Zc, Vr, σ_w	Zt, Zc, Vr, σ_w	Zt, Zc, Vr, σ_w	Zt
No. of Tilts	24 tilts	3 tilts	1 tilt	1 tilt	11 tilt	1
Elevations	0.3 to 24.7°	0.5 to 3.5°	0.3°	0.3° or lower	0.3 to 24.7°	0.3°
Max Range	256 km	113 km	2x113km	240 km	240km	256km
No. of Bins	256	226	226	960	960	2048
Scan time	5 min	4:30 min	30 s	50 s	~4 min	Up to ~21 min
Special		-0.5 to 0.0°	Random phase to retrieve second trip	Random phase to clean first trip echo	Random phase to clean first trip echo	Clear air high resolution and high quality scan
				Slow scan to remove low level ground clutter	Rapid scan for storm detection	

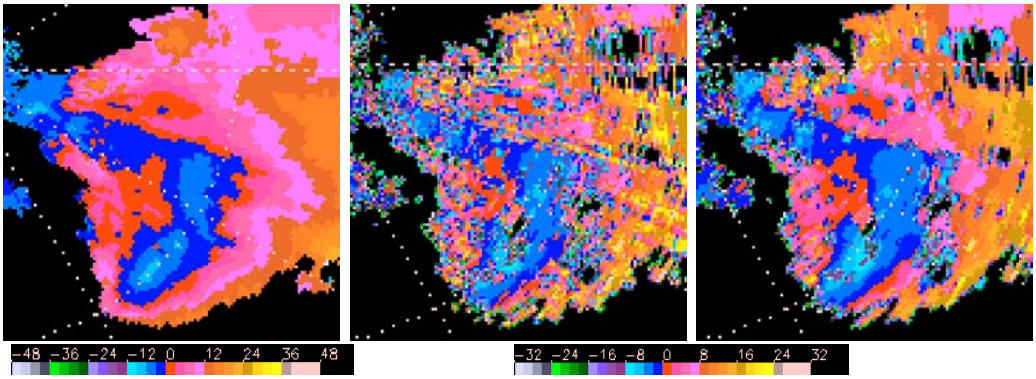

Figure 7: Three radial velocity images at 3.5° elevation angle of a convective thunderstorm. The range ring is drawn at 50 km range from the radar. The left most image is taken with dual PRFs of 1192:896 s^{-1} (or 16:12 m/s Nyquist velocity ratios or 4:3 PRF ratios). This has an extended Nyquist of 48 m/s and a maximum range of 113 km and uses the 0.8 μs pulse width. The data is clean and is used to verify the images on the right. The centre image is taken with dual PRFs of 600:480 s^{-1} (or 8.6:6.4 m/s or 5:4 PRF ratios). This has an extended Nyquist of 32 m/s with a maximum range of 240 km. The data is from an 11 elevation volume scan and uses the 1.27μs (instead of 0.8 μs) for greater sensitivity. The image is plagued with the expected dual PRF generated dealiasing errors. The image on the right despikes the errors using a simple median filter and produces a cleaner data set for further interpretation.

3. The Radar Network and Data

When the project began, the need for the network was analyzed. The siting of the radars was based on severe weather climatology, gaps in the existing network, population, and the NEXRAD radar coverage of portions of Canada (Fig. 1). Fig. 8 shows the types of analysis and GIS maps, which are used to determine the locations with the greatest combination of severe weather and population. Observed weather from synoptic observations was combined in a GIS system to produce maps that objectively ranks the location in terms of the observations. For example, wind and observed weather were linearly combined equally to produce maps which identified the distribution of the severe weather parameters

across Canada. The coastal regions and the downslope Chinook winds region show the greatest relative ranking. Another important parameter was population. The figure on the right of Fig. 8 shows the result of the GIS analysis where the various elements were subjectively weighted by different factors. In the end, the results are biased to be centred around the population centres. However, the analysis still indicates where the radars needed to be located in a relative sense.

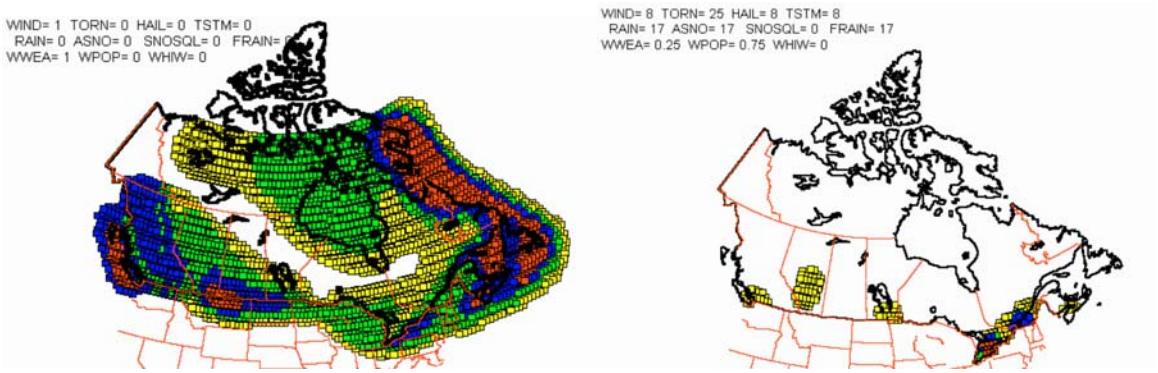

Figure 8: GIS analysis of wind and weather (left) synoptic observations and with population included (right). The figure shows the weightings used in the final analysis. The weightings are somewhat subjective but provide a relative objective rationale for the distribution of the radars. The shadings show the relative importance of the analysis in quartiles.

The network was designed to take advantage of the bordering NEXRAD radars. The NEXRAD NIDS data is acquired from a NOAAPORT satellite system at the Canadian Meteorological Centre in Dorval, Quebec (Jones and Gingras, 1999). This data is then broadcast via satellite (Canadian SATNET system) to Regional offices. This data is decoded by the radar processing software and is fully integrated with Canadian data or displayed individually.

Several of the radars are located on mountain sites. Negative elevation angles can be used in the Canadian network. Radiation analysis demonstrated that there is no health hazard from the radars (Stanley-Jones et al, 1999; Stuchly, 1999). A digital elevation model (DEM) is used in the analysis to determine the "optimal low level elevation angle". Fig. 9 shows the result of the analysis for the Val d'Irene radar located on the south shore of the St Lawrence River. The site is located on top of the Chic Choc Mountains and looks over the St Lawrence Valley to the north. The figure shows an azimuthal plot (abscissa) of the radar horizon in 0.5° increments and the colours indicate the height above ground at a range of 100km for the elevation angle shown on the ordinate scale. A 0.65° beam is assumed and the clear area above the horizon line represents the 3 dB beamwidth, above which good data is assumed to be collectable. In this case, an elevation of -0.5° provides usable data on low-level snow squalls in the St. Lawrence Valley (azimuth increment of ~100 to ~400). This has been well received by the operational community.

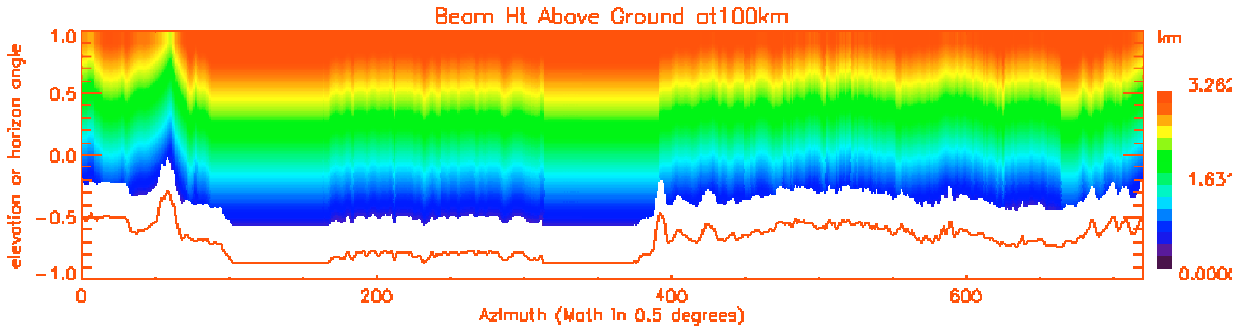

Figure 9: A horizon plot for the Val d'Irene radar to show how the lowest effective elevation angle is determined. The abscissa is the azimuth increment (0.5o azimuths) and the ordinate is the elevation angle. The plot shows the radar horizon but also the half-

beamwidth horizon used to show where "clean" data could be expected. The colours indicate the height of the beam at 100 km range for a given azimuth and elevation angle.

4. The Software Requirements

The requirements of the software are demanding. A single forecaster is responsible for providing severe weather warnings encompassing an area of up to eight radars - typically, a region of 3×10^6 km^2 - an area comparable to the size of Europe. Thirty or more forecasters cover a comparable area in the U.S. The Canadian forecaster must be able to maintain a broad view of the weather while at the same time be able to focus on individual thunderstorms. In addition, the type of severe weather across the country is quite varied.

In order to maintain surveillance and situational awareness over the entire forecast domain and to make warning decisions at the thunderstorm scale, a multi-radar composite approach was developed in which the forecaster could "drill down" to products either at a radar scale or at a thunderstorm scale. Philosophically, there has been a major paradigm shift in the radar processing from single radar to a network concept.

In addition, the plethora of radar products must be presented in a succinct fashion to allow rapid and decisive assessment of individual radar views of thunderstorms. Algorithmic products are used to identify severe thunderstorm features in the radar data. Thunderstorm scale "cell views" were developed to merge the various products. Another important aspect was to rank and classify all the storms across all the radars and present the information in a table, commonly called a Storm Classification, Identification and Tracking (SCIT) table (Johnson et al, 1998).

In any product-display system, it is always a balance between effective *products* versus viewing *functionality* and display *performance*. Since the products aren't perfect, interactive functionality must be built into the display of the system. Performance or the ability to do things quickly is of paramount importance. A platform independent Java based viewer application was developed to access and to interact with the radar products. To effectively use the limited screen space, the radar processing-viewer software was designed to use two high-resolution monitors. To effectively access a thunderstorm cell view product, "point and click/drill down" functionality was developed to link the composite, SCIT and cell view products. With some slightly reduced functionality, the radar products can be viewed on a common desktop computer.

To create the maximum flexibility in a wide variety of weather regimes, virtually all aspects of the system are user configurable including the severe weather classification rules. To maintain a watch on upstream and cross-border weather, the system ingests, processes and integrates the Level 3 data from the NWS WSR88D radars.

5. The CARDS System

Fig. 10 shows an overview of the flow of the radar data volume scans from radar to processing centre. The radars are connected to the radar processing centre on dedicated 128Kbaud links. In a few instances, satellite links are employed to move the data from the remote radar sites. There are five major radar processing centres for severe weather; these include Vancouver, Winnipeg, Toronto, Montreal and Dartmouth. The warning offices are not necessarily co-located with the processing centres. However, they are connected via T1 network links and the viewing software can access the radar server over the wide area network.

Figure 10: Data topology of the Canadian National Radar Network. The radar icons indicate the location of the radars. Solid lines indicate existing pathways for the volume scans and the dashed lines indicate future radar installations. Dash-dot lines indicate inter-Regional data flow paths. Note the ingest of NEXRAD data at the Canadian Meteorological Centre and the subsequent re-transmission to the Regions via SATNET. This figure also shows where the major radar processing and severe weather forecasting centres are located where a single forecaster provides the warning services.

Fig. 11 shows the processing at a Regional radar processing office. Multiple radar volume scans (including NEXRAD NIDS data) are ingested by the CARDS software. Two key elements of the software are that it is file based and that the science and graphics processing modules are split up. This allows the science processing and the image product processing to be distributed across Regions. Each science module creates a "metafile" product. For example, these metafile products may include fields of CAPPI's or EchoTops formatted in radar coordinate space and maintained at the volume scan data quantization resolution. These may also include outputs of the cell identification and mesocyclone algorithms, among others. One system can create the cell identification and classification metafiles to send to another system for display.

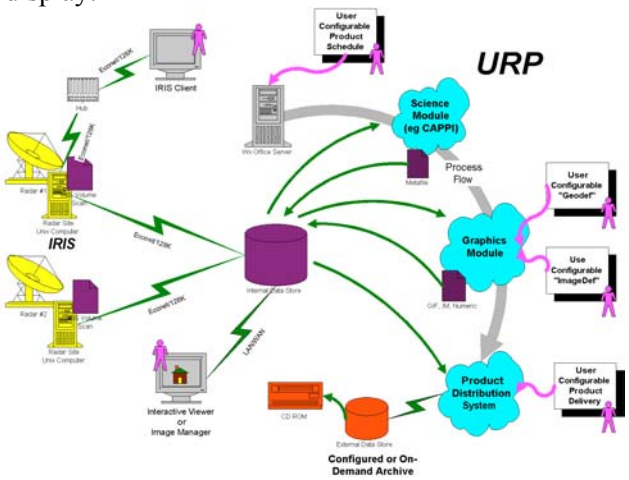

Figure 11: Schematic of the radar processing. The data flow and the processing is file based and makes use of the MSC TCP/IP intranet to distribute the data but also the radar processing. The algorithms can be processed in one location with the final products produced in another location.

Fig. 12 shows the "cell processing" specific to the severe weather aspects of the system. A MAXR metafile product from a single radar is created. This is thresholded, nominally at 45 dBZ, and a pattern vector feature identification technique (Zrnic et al, 1985) is used to identify thunderstorm cells. The average and maximum MAXR reflectivities and their locations (in latitude-longitude co-ordinates) are computed and stored in the CELLID metafile as well as the pattern vectors. These pattern vectors are used as a template or footprint and applied to other radar fields such as the echotop, VIL, etc and the

properties of the cell are computed and built up. At the end of the CELL PROPERTIES module, the storm cell is described by eight radar derived storm properties.

The next and major step is to merge the cells in the overlapping radar regions. If the same cell is identified on two radars, we select the cell that has the largest reflectivity value. Other criteria could have been chosen but at this first implementation and considering that attenuation at C Band can be significant, this selection criteria seem most reasonable. At the end of the CELL MERGE step, we have a data set of all the cells from a single time step for all the radars in the Regional composite. At this point we pass the data on to the TRACKER module which is based on the work of Dixon and Weiner (1993) to track the storms within and across radars.

Following the TRACKER, we assess the storm for severity. This is done in two ways - by rank and by classification. To compute the rank, we categorize the following parameters - the maximum reflectivity, the VIL density, max Hail size, max 45 dBZ echo top, the downdraft potential, mesocyclonic shear and BWER confidence - as detected, weak, moderate or severe by thresholds. These categories are assigned a numeric value from 1 to 4 and then summed to get an overall rank for the storm. To compute the classification (such as supercell), user configurable rules are implemented to combine radar detected features (such as existence of BWER, mesocyclone and alignment of the echo top over the low-level gradient). Note that in practice, the rank is more useful since it sorts all the storms in the entire Regional domain and across all the radars.

The ASSESSMENT CELL VIEW module then takes the output from the TRACKER and STORM ASSESSMENT and CLASSIFICATION (SAC) module and creates the metafile for the SCIT table and the image metafiles of individual thunderstorm cells. A single image product is created to allow the forecaster to diagnose the cell for severity (Fig. 15). All of the products are configurable.

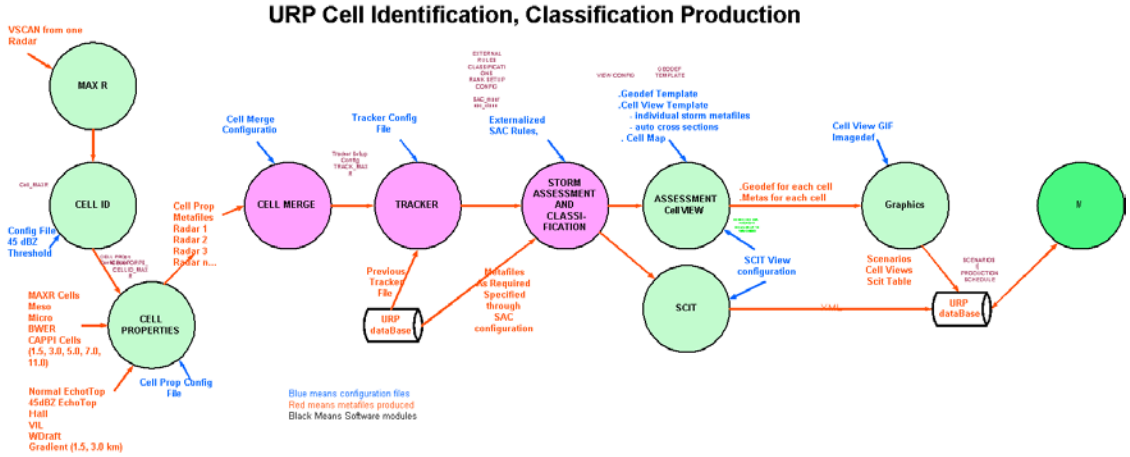

Figure 12: Thunderstorm cell to SCIT and Cell View processing. The new aspects to this processing chain are the merging and tracking of cells across radars, the configurable rules to rank and assess storms, the configurable SCIT and CELL VIEW products and the ability to use a platform independent viewer to view the radar data. See text for more details.

THE INTERACTIVE VIEWER

The user interface to the products is absolutely critical. The functionality and performance of the user interface must match the products and interaction concept. To reduce the use of screen real estate and to increase the usability, all products can be created as multi-radar composites and these products are layered in the viewer so that the user can toggle instantly from one product to another. A platform

independent JAVA application called the Interactive Viewer (IV) was created. This uses interactive web technology to serve and interact with the image products in the CARDS database.

The usual animation, pan and zoom features are available. Other functionality of the IV include the ability to draw lines (grease pencil), do manual extrapolations, do cross-sections, add text, access single radar products, drill down to access cell views and to toggle between products and backgrounds.

HARDWARE

The server processing system is a collection of LINUX Intel computers configured as a cluster. The front end of the cluster is a dual CPU 1.26GHz with 1Gbyte of RAM. This does most of the scientific processing. The back end of the cluster is a collection of similar machines. The primary purpose of the back ends is to generate the graphical images. The generation of the images places the greatest workload on the hardware and this is addressed by adding processors to the "back end"

The IV is an application that uses the existing LINUX based display workstation in the forecast office. It can also be used on a Windows machine. The main requirement is that the machine has 512Mbyte or more of memory but this is dependent on the product sizes. Typically, in the MSC Regional operational environment, the Regional composites are 2000x1600 pixel images and so they drive the memory requirements. A dual monitor with single logical screen configuration is recommended.

DEMONSTRATION OF CAPABILITY

Fig. 13 shows a typical Regional composite. The size of the composite is 2000x1600 pixels with ~1km per pixel resolution. The forecaster will typically leave this product up on a single monitor to maintain situational awareness. The forecaster can then zoom and pan on this image to focus on the area of interest. Circles and lines indicate cells and tracks. The cells are colour coded based on the rank weight. The figure shows a grey scale topography background. Lightning and the NEXRAD radars are included.

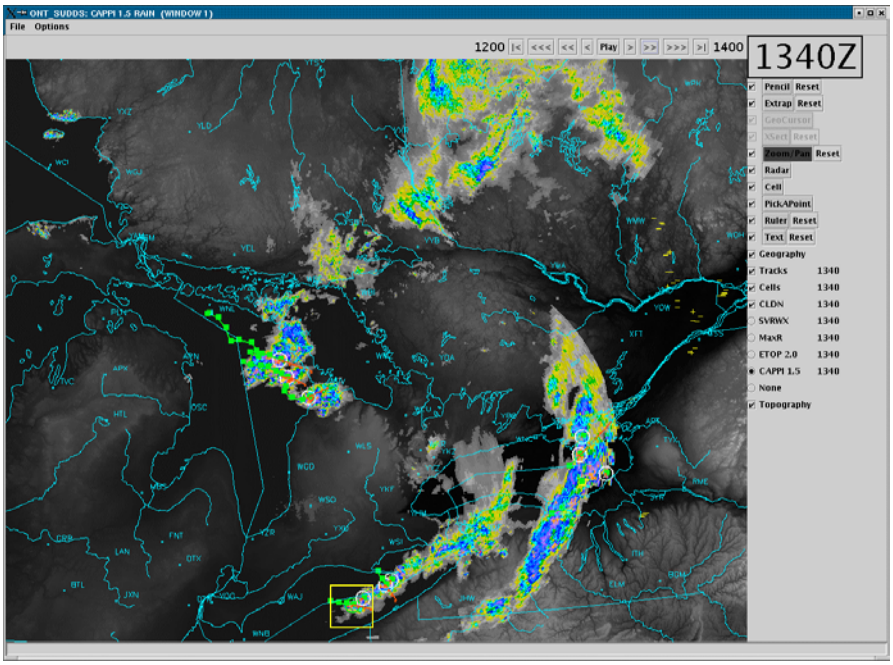

Figure 13: An example of a Regional composite. This is the typical size of the domain used at the Ontario Forecast Centre (~2000kmx1600km). The image shows a zoomed image of the cells, tracks and lightning strikes. Eight Canadian radars and 12

US radars contribute to the image. Note the cells and tracks. The square box shows how the user interactively "selects" a cell for diagnosis.

Fig. 14 shows a SCIT table. The composite and the SCIT table products are invoked and displayed at the same time. The forecaster can either drill down to a CELL VIEW (Fig. 15) into a storm via the composite or via the SCIT table. She/he can also rapidly survey the cells from the SCIT table without invoking the CELL VIEW products by right clicking on the SCIT or on the composite and appropriate SCIT entry or cell is highlighted.

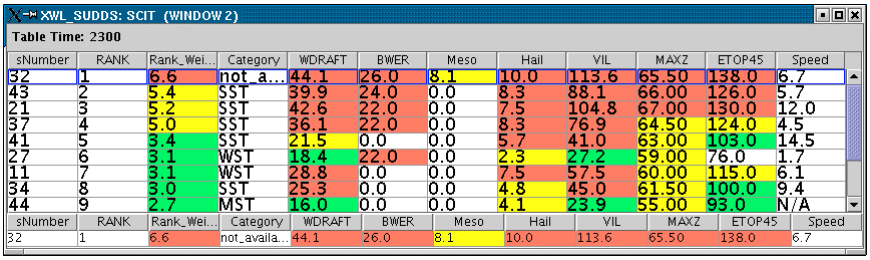
XWL_SUDDS: SCIT (WINDOW 2)

Table Time: 2300

sNumber	RANK	Rank_Wei...	Category	WDRAFT	BWER	Meso	Hail	VIL	MAXZ	ETOP45	Speed
32	1	6.6	not_a...	44.1	26.0	8.1	10.0	113.6	65.50	138.0	6.7
43	2	5.4	SST	39.9	24.0	0.0	8.3	88.1	66.00	126.0	5.7
21	3	5.2	SST	42.6	22.0	0.0	7.5	104.8	67.00	130.0	12.0
37	4	5.0	SST	36.1	22.0	0.0	8.3	76.9	64.50	124.0	4.5
41	5	3.4	SST	21.5	0.0	0.0	5.7	41.0	63.00	103.0	14.5
27	6	3.1	WST	18.4	22.0	0.0	2.3	27.2	59.00	76.0	1.7
11	7	3.1	WST	28.8	0.0	0.0	7.5	57.5	60.00	115.0	6.1
34	8	3.0	SST	25.3	0.0	0.0	4.8	45.0	61.50	100.0	9.4
44	9	2.7	MST	16.0	0.0	0.0	4.1	23.9	55.00	93.0	N/A

sNumber	RANK	Rank_Wei...	Category	WDRAFT	BWER	Meso	Hail	VIL	MAXZ	ETOP45	Speed
32	1	6.6	not_availa...	44.1	26.0	8.1	10.0	113.6	65.50	138.0	6.7

Figure 14: An example of a SCIT. The colour coding indicates the categorical ranking. The extra line at the bottom highlight the data for the selected cell.

Fig. 15 shows a CELL VIEW product. This shows a variety of images that allow the forecaster to quickly make a decision as to the severity of the storm. There are two CELL VIEW images created for each storm - one based on reflectivity and one based on Doppler data. The product shows an ensemble product of the algorithms (upper left hand corner), automatically determined cross-sections, four CAPPIs (1.5, 3.0, 7.0, 9.0 km), reflectivity gradient, MAXR, echo top, VIL density, Hail, BWER and 45 dBZ echo top and time graphs. The ensemble product shows the outputs of all the algorithms plus the low level CAPPI as a simplified image and a MAXR product as a contour product to show the overhang, a common and defining feature of a severe storm.

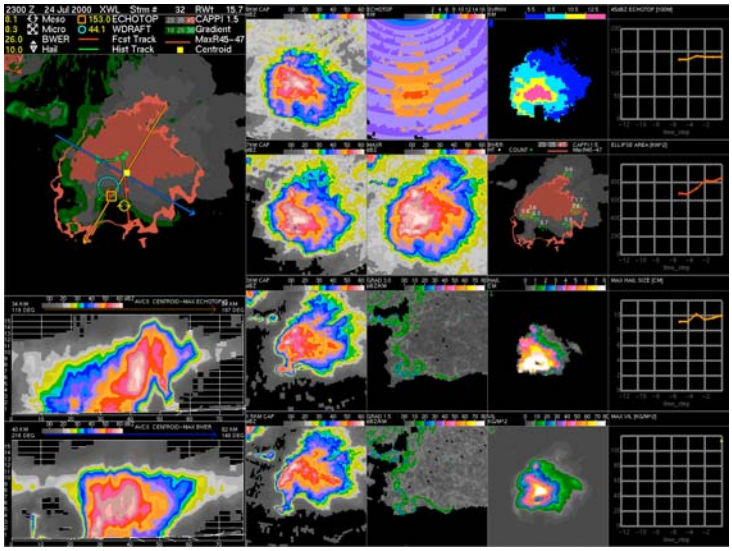

Figure 15a: An example of a CELL VIEW. An ensemble of the algorithm outputs is displayed in the upper left hand corner showing their relative locations. Automatic cross-sections (lower left) show the vertical structure of the storm. CAPPI's of various heights and other plan products are used to diagnose the severity of the storm. Time height graphs show the time evolution of the storm.

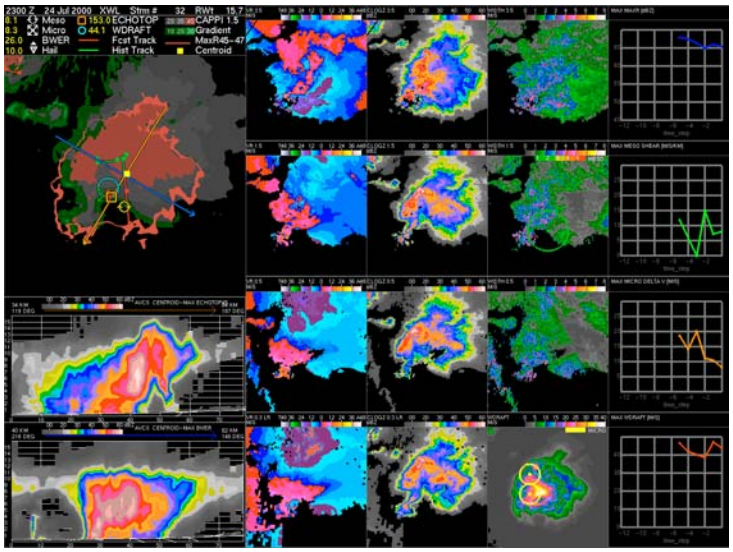

Figure 15b: An example of a CELL VIEW. The left hand side is similar to the previous figure. In this product, radial velocity imagery is displayed. Note the microburst detection algorithm is overlaid on the gust potential product.

6. Maintenance and Life Cycle Management

The on-going operation of the expanded network presents its own challenges. The radars are managed and funded as a separate network. An Integrated Logistics Support document has been prepared to document the tasks of those involved in supporting the network. This addresses issues such as the maintenance process; the qualifications of all staff involved; system test and support equipment calibration; training of both the maintainers and data users; and the technical data of various kinds.

The radars are on the Meteorological Service of Canada intranet and report the status of many parameters every minute. Software (Fig 16) displays the status of all radars and allows maintainers to identify problems and to correct many of them remotely. Statistics show that we have achieved an "up-time", on average, over 96% and the highest monthly "up-time" reported at 98.7%.

Fig 16 Radar Monitoring output showing radar status over 48 hours based on 1 and 10 min. data. The entire network can be monitored and in many cases problems can be corrected over the TCP/IP intranet.

The radars are routinely calibrated against known references. Current best efforts to maintain an accurate calibration have not resulted in consistent measurements between radars. This is being addressed as a documentation and training issue. Development of routines to do inter-radar real time comparison is in progress. We also intend to experiment with calibration of at least portions of the system against known sources such as the sun.

7. Summary

This paper presents a snap shot of the Canadian National Radar Project. The project is near the end of its planned six years. The project is under budget and on time in spite of the scope changes. The mandate for our radar systems has expanded from severe weather applications, to include hydrology, data assimilation, model verification, aviation, commercial and others. An in-house approach has been adopted to both the hardware and the software development and implementation. The wide mandate for the radars necessitates that this evolutionary approach be adopted as the new and future users of the radar data have different degrees of maturity in their requirements.

The radar system is viewed as a network. The network and software capabilities will evolve as the science and the software develops over time, as this new concept becomes refined and as new clients are able to define their requirements. A consequence of this philosophy and the multiple radars per office working scenario, multi-layered composite radar imagery will be the standard "bread and butter" product for forecasting. Having the volume scan data from multiple radars available, a network approach to radar data processing can now be developed. For example, multiple radar approaches to attenuation correction are therefore now feasible and this will be the development path in the next version of the software processing. Radar calibration is a major concern. It may be more important to be consistent rather to be accurate though both are desirable.

The version of the software, presented in the paper, addresses many of the needs of the Canadian severe weather forecaster. There are several innovations - network radar processing, multi-cell merging, ranking, and classification - that require extensive tuning to function in the diverse weather regimes across the country. In the operational implementation, upstream CAPPI and Echotop product metafiles are transferred from one region to another for inclusion in the downstream composite to create, in concept, a distributed but integrated national radar processing system.

8. References

Crozier, C.L., P. Joe, J.W. Scott, H.N. Herscovitch and T.R. Nichols, 1991: The King City operational Doppler radar: development, all season applications and forecasting, *Atmosphere-Ocean*, 29, 479-516.

Dixon, M. and G. Weiner, 1993: TITAN, Thunderstorm Identification, Tracking, Analysis and Nowcasting - A Radar-based Methodology, *JAOT*, 10, 785-797.

Gingras, Y. and Jones, R.,1999: Processing of North American Radar Networks Data at the Canadian Meteorological Centre, *29th Conf. Radar Met., Montreal, AMS,* 331-334.

Joe, P., D. Hudak, C. Crozier, J. Scott, R. Passarelli Jr., A. Siggia, 1998: Signal Processing and Digitial IF on the Canadian Doppler Radar Network, *Advanced Weather Radar Systems, COST 75 International Seminar,* Locarno, Switzerland, 23-27 March , 544-556.

Joe, P. and P.T. May, 2002: Practical Operations and Data Characteristics of Dual PRT Weather Radars, *Accepted for publication in JAOT.*

Johnson, J.T., P.L. MacKeen, A. Witt, E. D. Mitchell, G. J. Stumpf, M. D. Eilts, and K. W. Thomas, 1998: The Storm Cell Identification and Tracking Algorithm: An Enhanced WSR-88D Algorithm. *Wea. and Forecasting,* 13(2) 263-276.

Lapczak, S., E. Aldcroft, M. Stanley-Jones, J. Scott, P. Joe, P. Van Rijn, M. Falla, A. Gagne, P. Ford, K. Reynolds and D. Hudak, 1999: The Canadian National Radar Project, *29th Conf. Radar Met., Montreal, AMS,* 327-330.

Marshall, J.S. and E.H. Ballantyne, 1975: Weather Surveillance Radar, *J.A.M., 14, 1317-1338.*

May, P.T. and P. Joe, 2001: The production of high quality Doppler velocity fields for dual PRT weather radar, *30th Conf. Radar Met., Munich, AMS,* 286-288.

Stanley-Jones, M.L., J. Scott, R. Young and A.E. Aldcroft, 1999: Environment Canada CWSR-98A and CWSR-98E/R Weather Radars, Microwave Radiation Analysis Report, (internal MSC document), 25pp.

Stuchly, M.A., 1999: Review of Environment Canada CWSR-98A and CWSR-98E/R Weather Radars, Microwave Radiation Analysis Report, Revision 4.1 (internal MSC document), 3pp.

Zrnic, D.S., D. Burgess and L. Hennington, 1985: Automatic Detection of Mesocyclonic Shear with Doppler Radar, *JAOT*, 2, 425-438.